Int. J. Heat Mass Transfer. Vol. 21, pp. 1069–1080

0017-9310/78/0801-1069 $02.00/0

EXPERIMENTS ON HEAT TRANSFER AND PRESSURE DROP FOR A PAIR OF COLINEAR, INTERRUPTED PLATES ALIGNED WITH THE FLOW

N. CUR and E. M. SPARROW
Department of Mechanical Engineering, University of Minnesota, Minneapolis, MN 55455, U.S.A.

(*Received* 5 *December* 1977 *and in revised form* 27 *January* 1978)

Abstract—Experiments have been performed to determine the heat-transfer characteristics for each plate of a two-plate colinear array aligned parallel to the flow direction and situated in an airflow in a flat rectangular duct. The pressure drop associated with the plates was also determined. The plate thickness and the inter-plate spacing were parametrically varied (for a fixed plate length), as was the Reynolds number. It was found that while the Nusselt number may either increase or decrease with plate thickness, depending on the operating conditions, it should increase for conditions corresponding to those commonly encountered in an interrupted-plate heat exchanger. The pressure drop increase caused by increasing plate thickness is greater than the largest thickness-related increase of the Nusselt number. The presence of the inter-plate gap affects the Nusselt numbers for both the first and second plates, but to a greater extent for the latter. In many cases, the curves of Nusselt number vs spacing attain a local maximum and indicate that the conventional spacing-to-length ratio of unity is not necessarily optimal.

NOMENCLATURE

- A, sublimation surface area of plate;
- D_h, hydraulic diameter for flow space above or below plate, equation (2);
- $\mathscr{D}$, naphthalene–air diffusion coefficient;
- h, height from plate surface to duct wall, Fig. 1;
- K, mass-transfer coefficient, equation (1);
- L, plate length;
- M, rate of mass transfer from plate;
- Nu, Nusselt number;
- Pr, Prandtl number;
- Δp, pressure drop due to plate array, Fig. 14;
- Re, Reynolds number, equation (3);
- S, inter-plate spacing;
- Sc, Schmidt number;
- Sh, Sherwood number;
- t, plate thickness;
- $\bar{V}$, mean velocity in space above or below plate;
- $\dot{W}$, mass flow rate through duct;
- w, duct width;
- x, axial distance along duct.

Greek symbols

- μ, viscosity;
- ν, kinematic viscosity;
- ρ_n, density of naphthalene vapor;
- ρ, air density.

INTRODUCTION

A COMMONLY used technique for obtaining improved performance of heat exchange devices is to employ heat-transfer surfaces that are periodically interrupted along the streamwise direction. Such an arrangement may be viewed as a succession of colinear plate segments aligned parallel to the flow, with gaps between the successive plates. Each gap enables the velocity and temperature distributions, which were developed in the boundary layer on the plate segment upstream of the gap, to become more homogeneous. When the thus-homogenized flow encounters the next plate, new boundary layers develop, but their growth is limited by the next gap. The relatively thin boundary layers that are obtained by the use of interrupted surfaces is the key factor in the high heat-transfer effectiveness of such surfaces.

Overall heat-transfer and friction characteristics of full scale heat exchanger models which incorporate the interrupted-surface concept have been reported in the published literature (e.g. [1–4]). These data are of direct utility in the design of specific heat exchange devices. However, because they were obtained from overall performance tests, the data do not provide insights into the complex processes which stem from the presence of the interruptions. It appears that the only prior experimental study dealing with the heat-transfer characteristics of individual plate segments was not published in the archival literature; rather, it was one of a series of reports from the mechanical engineering department of Stanford University [5]. Its existence became known to the present authors only during the later stages of the research that is being reported here. The complementary aspects of the present research and that of [5] will be elaborated shortly.

The present experiments were undertaken to obtain more detailed information about the heat transfer and pressure drop characteristics of interrupted heat transfer surfaces than had been heretofore available. As shown schematically in Fig. 1, the basic configuration consisted of two colinear plates aligned with the flow direction. The plates were situated in a flat rectangular duct (5:1 aspect ratio) with an upstream hydrodynamic development length to ensure fully de-

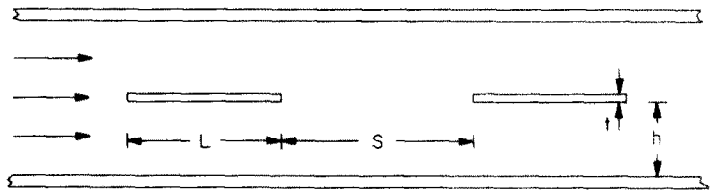

FIG. 1. Schematic diagram of the colinear plate array.

veloped flow at the test section. By varying the plate thickness t and plate-to-plate spacing S, the thickness–length ratio t/L was assigned values of 0.04, 0.08, and 0.12, while the spacing ratio S/L ranged through 0, 0.25, 0.5, 1, and 2. In addition to these geometrical parameters, the Reynolds number was varied from about 1000–14000. Air was the working fluid for the experiments.

The inclusion of t/L as a parameter of the experiments was motivated by conditions that prevail in compact heat exchangers. As heat exchangers are made more compact, there is a general shrinking of dimensions, but the thickness cannot be reduced below a basic minimum necessary for structural integrity. Although the absolute thickness of the plates in highly compact heat exchangers is small, it may not be negligible relative to the plate length L. The t/L range employed here is typical of that encountered in practice. In addition, the Reynolds number range was selected to reflect that of compact heat exchangers.

Two complementary sets of experiments were performed. In one set, both the first and the second plates were active heat- (mass-) transfer surfaces. On the other hand, for the other set, heat (mass) was transferred only at the second plate, with the role of the first plate being confined to its hydrodynamic effects. These studies were undertaken to identify the sensitivity of the second-plate transfer processes to possible upstream temperature (concentration) build-ups.

To facilitate the research, cognizance was taken of the analogy between heat and mass transfer, and mass-transfer experiments were performed in lieu of heat-transfer experiments. The naphthalene sublimation technique was employed for the mass-transfer experiments, with air as the working fluid. The plates pictured in Fig. 1 were naphthalene-coated metal substrates, and the mass-transfer rates were determined by direct weighing of the plates both before and after a data run. In addition, the duct was heavily instrumented with pressure taps.

The mass-transfer results will be reported in terms of the Sherwood number which, by analogy, is equal to the Nusselt number. The presentation of results is structured so that the responses of the Sherwood number to variations in the thickness, the spacing, and the Reynolds number are separately exhibited. The pressure drop, made dimensionless by the velocity head, is also reported as a function of these parameters.

The experiments of [5], also for a two-plate array, encompassed heat transfer measurements but not pressure drop. Since the plates were positioned just downstream of a plane-walled convergent nozzle which fed a 3:2 rectangular duct, the velocity in the approach flow differed from the fully developed duct flow of the present experiments. Two spacing ratios, $S/L = 0.5$ and 1, were investigated and, presumably because of this limited range, the effect of spacing was not explicitly delineated in the presentation of results. Although three plate thicknesses were employed ($t/L = 0.03$, 0.06, and 0.10), the effect of thickness was also not explicitly displayed. This may well have been due to the fact that only two of the thicknesses ($t/L = 0.06$ and 0.10) shared a common leading/trailing edge configuration (i.e. blunt); the $t/L = 0.03$ plates had tapered leading and trailing edges. Some comparisons between the present results and those of [5] will be presented later.

Also of relevance is the flow visualization study reported in [6], which also dealt with a two-plate array. With the aid of dye injection and the hydrogen bubble technique, the flow field was observed in the inter-plate gap and adjacent to the second plate. Owing to the wake shed by the first plate, oscillatory unsteady flows prevailed above a threshold value of a wake-width Reynolds number, with vortices in evidence under some conditions. Measurements with a hot-film probe situated adjacent to the leading edge of the second plate revealed that the amplitude of the oscillating velocity did not vary monotonically as the inter-plate spacing S was increased. Rather, the amplitude displayed a succession of peaks and valleys as a function of S. Of particular interest was the finding that the presence of the second plate can have a marked influence on the wake of the first plate. The results of [6] affirm the complexity of the flow field.

THE EXPERIMENTS

Experimental apparatus

The key component of the experimental apparatus was a horizontal rectangular duct having a 5:1 cross sectional aspect ratio (width $\times$ height) and an overall length of 62 hydraulic diameters. The upstream portion of the duct (37 hydraulic diameters) served as a hydrodynamic development length, with the test section and the downstream redevelopment length constituting the remainder of the duct. At its exit, the duct interfaced with a rectangular-to-circular transition piece, which connected to an orifice metering section. In turn, the orifice-section pipe was coupled to a blower situated outside the laboratory room. The duct cross sectional dimensions were 133.5 $\times$ 26.7 mm (5.25 $\times$ 1.05 in), with a hydraulic diameter of 44.5 mm (1.75 in).

The test section was designed to permit rapid installation and removal of the naphthalene-coated test plates and to ensure precise, positive positioning of the plates. The rapid installation and removal minimizes extraneous sublimation of the naphthalene. To this end, the upper wall of the test section (an axial length of about 13 hydraulic diameters) was made removable. When in place, this section of the wall was held fixed by six quick-release clamps, and a leak-proof seal was accomplished with the aid of O-rings. To gain access to the test section, the clamps were released and the wall removed, all in a matter of seconds. The closing of the test section could be accomplished in a similarly short time.

To facilitate the positioning and support of the test plates, the upper portion of each of the side walls was recessed so as to create a ledge that ran the entire length of the test section. Each test plate was installed so that its spanwise extremities [a 9.5 mm (3/8 in) uncoated length at each end of the plate] lay on the respective ledges. The plate was positively positioned by pins. Once both test plates had been installed, a precisely machined bar was inserted so as to fill each side-wall recess. The thus-reconstituted side wall presented a smooth, flat surface to the flow.

Axial pressure distributions were measured with the aid of 23 taps deployed along the spanwise centerline of the upper wall. The tap locations will be evident from the pressure distribution results to be presented later. The pressure signals were sensed by a Baratron capacitance-type meter whose output could be read to 0.0001 mm Hg. For the measurement of the flow rate through the duct, calibrated orifice plates were used in connection with a manometer. To provide a well defined inlet condition for the flow entering the duct, the entrance plane was framed with a large baffle plate whose upstream face was flush with the exposed edges of the duct walls.

Further information about the apparatus is available in the thesis [7] on which this paper is based.

Naphthalene-coated test plates

Each test element was a sandwich-like composite made up of a metal plate (i.e. the core) whose surfaces were coated with a thin layer of naphthalene. A substantial amount of development work was needed in order to devise procedures for producing naphthalene coatings of high surface quality. The approach finally adopted consists of a combination of casting and machining, the general features of which will be outlined here—with further details in [7].

The metal plates were of mild steel and rectangular in shape, 25.4 × 152.4 mm (1 × 6 in). The naphthalene coating covered a 25.4 × 133.4 mm (1 × 5.25 in) surface area, with the uncoated portions situated adjacent to the two extremities. As noted earlier, these uncoated portions were inserted into recesses in the duct side walls and thereby served to support and position the plate during the experiment. Naphthalene coatings were applied to both faces of the metal plates, but not to the edges. The leading and trailing edges of the plates were squared off and, therefore, appeared blunt to the flow.

Three sets of test plates were employed, respectively with metal substrate thicknesses of 0.71, 1.73, and 2.74 mm (0.028, 0.068, and 0.108 in). The naphthalene coating applied to each face of a given plate was about 0.15 mm (0.006 in) thick. Therefore, the overall thicknesses of the respective sets of plates were 1.01, 2.03 and 3.04 mm (0.040, 0.080, and 0.120 in). These resulted in ratios of thickness to streamwise length t/L of 0.04, 0.08, and 0.12.

To prepare for the coating process, the faces of each metal plate were lightly sandblasted to aid the adhesion of the naphthalene. To provide further anchoring of the naphthalene, an array of small holes were drilled adjacent to all the edges of the plate, all around the coated perimeter; these holes were filled with molten naphthalene during casting. Subsequent to these machining operations, the metal plates were painstakingly straightened to compensate for any bending which might have occurred when residual stresses were unlocked during sandblasting.

For the casting, the surface of the metal plate to be coated was placed horizontally, facing upward, and then framed with metal bars so as to form the sides of a mold. Molten naphthalene was poured into the mold through the open top to a depth of about 2.5 mm (0.1 in) and allowed to cool. The plate was then turned over and a poured naphthalene coating applied to the other face. A machining procedure, performed with a vertical milling machine and a fly-cutter attachment, was employed to obtain a naphthalene coating of the desired thickness (~ 0.15 mm) and surface finish.

Several plates were prepared in one batch in order to enable a succession of data runs to be performed in a given day. When the machining was completed, the coated plates were sandwiched between glass plates and wrapped in plastic to minimize sublimation. The plates were then placed in the laboratory to attain thermal equilibrium. All aspects of the casting and machining process were performed with a high standard of cleanliness to avoid contamination of the surface of the coating.

As noted earlier, some experiments were performed in which only the second plate participated in the mass transfer process. In those experiments, the first plate was a mild steel plate with a thickness equal to the total thickness (metal plus coatings) of the corresponding mass transfer plates.

Experimental procedure

Air was drawn into the apparatus from the temperature-controlled ($\sim 20°C$), windowless laboratory room and was exhausted at the roof of the building. The outside exhaust ensured that the concentration of the naphthalene vapor in the entering air was zero, while the positioning of the blower in a service corridor outside the laboratory avoided thermal disturbances.

The amount of naphthalene sublimed during a data run was determined from measurements of the mass of

the test plates made immediately before and immediately after the run. The measurements were performed with a precision balance having a smallest scale division of 0.1 mg. The duration of a run was selected so that the change in the mean thickness of each film would be about 0.018 mm (0.0007 in). Duration times ranged from 20 min to 2 h, depending on the Reynolds number. The change of mass during a run typically fell in the range 100–150 mg.

Auxiliary experiments were performed to assess the possible extraneous loss of mass which might have occurred during the installation and removal operations and the weighing of the test plates. Typically, the extraneous loss was on the order of 2%, and an appropriate correction was made.

Data reduction

The measured mass loss and the duration time of a data run yielded the mass-transfer rate $\dot{M}$ per plate. With this, a mass-transfer coefficient K and its dimensionless counterpart, the Sherwood number Sh, were evaluated

$$K = \frac{\dot{M}/A}{\rho_{nw} - \rho_{n\infty}}, \quad Sh = \frac{KD_h}{\mathscr{D}}. \tag{1}$$

The area A appearing in the definition of K is the total naphthalene surface area per plate, whereas ρ_{nw} and $\rho_{n\infty}$ respectively represent the naphthalene vapor concentrations at the surface and in the free stream. The former was evaluated from the Sogin vapor pressure–temperature relation [8] in conjunction with the perfect gas law.

The free stream concentration for the first plate is zero, and it is also zero for the second plate when the first plate is non-subliming (i.e. uncoated). When the first plate is subliming, the distribution of the naphthalene vapor in the stream approaching the second plate depends on the degree of mixing in the interplate gap, and it is difficult to establish the free stream concentration with any degree of certainty. In view of this, $\rho_{n\infty}$ was taken to be zero for all cases. Thus, comparisons of K (or Sh) among the various cases is equivalent to a comparison of mass-transfer rates (for a given surface concentration).

The hydraulic diameter D_h appearing in the Sherwood number pertains to the flow space either above or below a plate (see Fig. 1). It was felt that this flow space is more relevant to the problem at hand than the entire cross section of the duct. If w denotes the spanwise width of the duct (normal to the plane of Fig. 1), then

$$D_h = 4hw/(2w+2h). \tag{2}$$

The diffusion coefficient $\mathscr{D}$ was evaluated via the Schmidt number $Sc = \nu/\mathscr{D}$ with $Sc = 2.5$ [8] and ν as the kinematic viscosity of air.

The Reynolds number used to parameterize the results is also based on the flow space above or below a plate. If $\dot{W}$ represents the total mass flow through the duct, then $\dot{W}/2$ passes through the spaces above and below a plate. Then, if $\bar{V}$ is the mean velocity in these flow spaces,

$$Re = \bar{V}D_h/\nu = 4(\dot{W}/2)/\mu(2w+2h). \tag{3}$$

It should be noted that the Reynolds number defined by equation (3) is smaller by about a factor of two than the Reynolds number for the duct cross section as a whole. Thus, whereas the range of Re for the experiments extended from about 1100 to 13 600, the duct Reynolds number ranged from 2000 to 25 000.

RESULTS AND DISCUSSION

The presentation of the mass-transfer results will be made in three parts, respectively with the Reynolds number, the thickness ratio, and the spacing ratio as the abscissa variable. With a view to generalizing the results, the quantity $Sh/Sc^{0.4}$ is plotted on the ordinate in all the figures rather than Sh itself. The choice of $Sc^{0.4}$ as the scale factor rather than $Sc^{1/3}$ (as in the Colburn j-factor) was based on two considerations. First, the dependence of Nu on Pr (or of Sh on Sc) is, according to the most recent duct flow correlations (e.g. [9]), at least to the 0.4 power in the range of intermediate Pr (say, 0.7–2.5). Second, consistently better correlation between naphthalene sublimation results ($Sc = 2.5$) obtained in our laboratory for a variety of flows and corresponding heat-transfer results for air ($Pr = 0.7$) has been attained with $Sc^{0.4}$ than with $Sc^{1/3}$.

According to the analogy between heat and mass transfer, a Nusselt–Reynolds–Prandtl correlation should be identical to a Sherwood–Reynolds–Schmidt correlation. Therefore, the ordinates of the figures have a dual label, $Sh/Sc^{0.4}$ and $Nu/Pr^{0.4}$. In the presentation that follows, the words heat transfer and mass transfer, as well as other corresponding pairs of words, will be used interchangeably.

Nusselt number–Reynolds number presentation

The heat/mass-transfer results, plotted as a function of the Reynolds number, are presented in Figs. 2–5. The consecutive figures correspond to spacing ratios S/L of 0.25, 0.5, 1, and 2. Results for $S/L = 0$ (plates touching) are omitted because of space limitations but may be found in [7]. In each figure, there are three groupings of curves which respectively correspond to the first plate, to the second plate (with mass transfer at the first plate), and to the second plate when there is no mass transfer at the first plate. The latter group of curves also correspond to an unheated first plate in the analogous heat-transfer situation, and this designation appears in the figures. Within each group, there are three curves, respectively for thickness ratios t/L of 0.04, 0.08, and 0.12.

Aside from the expected trend whereby the Nusselt number increases with increasing Reynolds number, the figures contain a variety of complex results. If attention is focused on the first plate, it is seen that there is a pattern which is consistent for all of the spacings. In the range of lower Reynolds numbers, the Nusselt number decreases somewhat with increasing

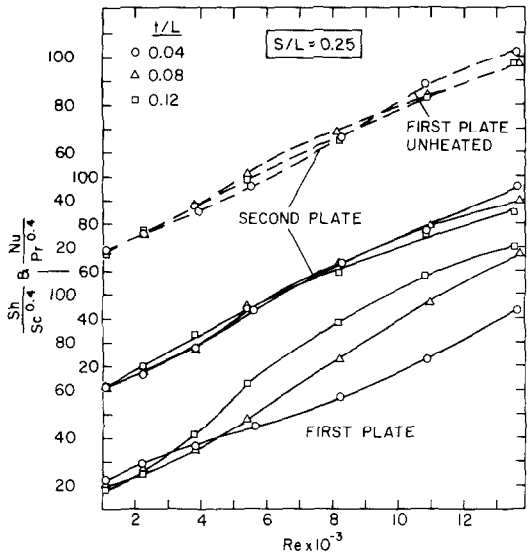

FIG. 2. Nusselt/Sherwood number variation with Reynolds number; inter-plate spacing ratio $S/L = 0.25$.

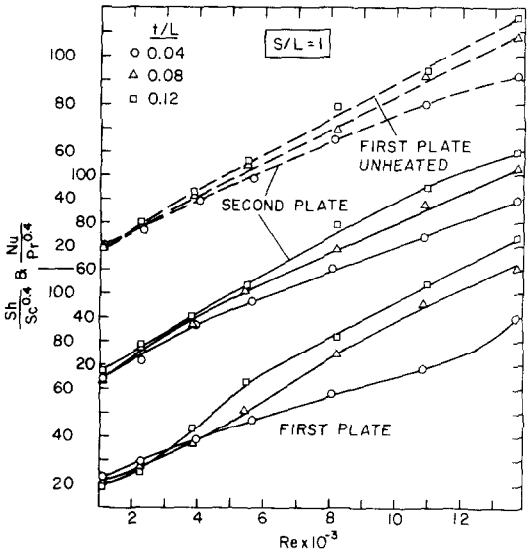

FIG. 4. Nusselt/Sherwood number variation with Reynolds number; inter-plate spacing ratio $S/L = 1$.

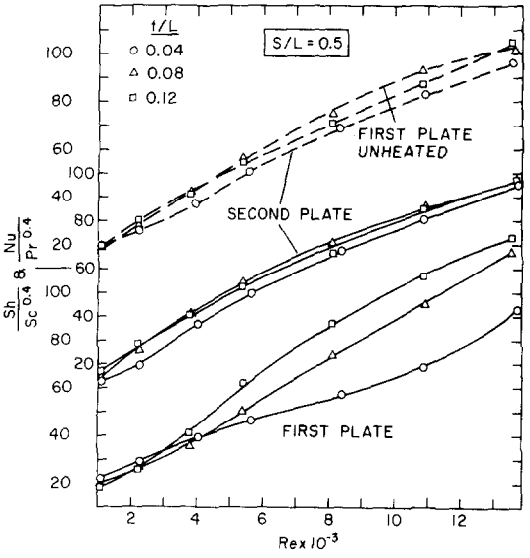

FIG. 3. Nusselt/Sherwood number variation with Reynolds number; inter-plate spacing ratio $S/L = 0.5$.

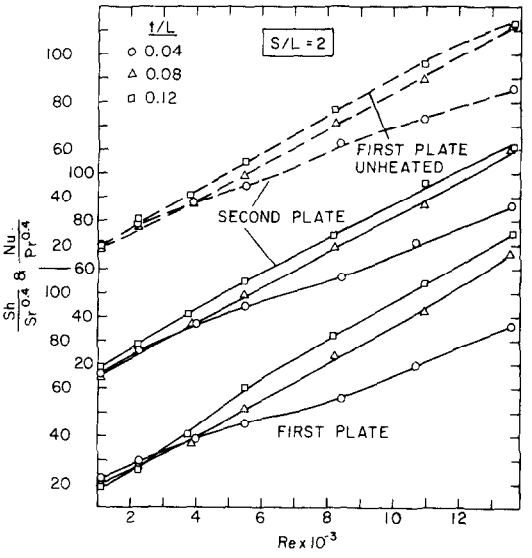

FIG. 5. Nusselt/Sherwood number variation with Reynolds number; inter-plate spacing ratio $S/L = 2$.

plate thickness. On the other hand, at higher Reynolds numbers (i.e. over most of the range studied here), the Nusselt number increases substantially with plate thickness.

Thus, with regard to the heat-transfer performance of the first plate, the thickness effect plays a different role in different ranges of the Reynolds number. The lower Nusselt numbers that occur for thicker plates at lower Reynolds numbers are probably due to the sluggish separation bubbles that are created by the leading edge bluntness. At higher Reynolds numbers, vortices and disturbances shed by the blunt leading edge increase the turbulence level and may cause the boundary layer to go turbulent. These factors contribute to an increase of the Nusselt number with increasing plate thickness.

The trends for the second plate are quite different from those for the first plate. At small spacings, the Nusselt numbers for the second plate are quite insensitive to thickness over the entire Reynolds number range. This appears to be reasonable, since for small spacings the first plate screens the blunt leading edge of the second plate from direct impingement by the oncoming flow. As the spacing increases and greater homogenization of the flow occurs in the inter-plate gap, the sensitivity of the Nusselt number to thickness increases and tends to approach that of the first plate. For $S/L = 1$, which is commonly encountered in heat exchangers, the second-plate results, relative to those for the first plate, are less responsive to thickness and, in addition, the reversal at lower Reynolds numbers does not occur.

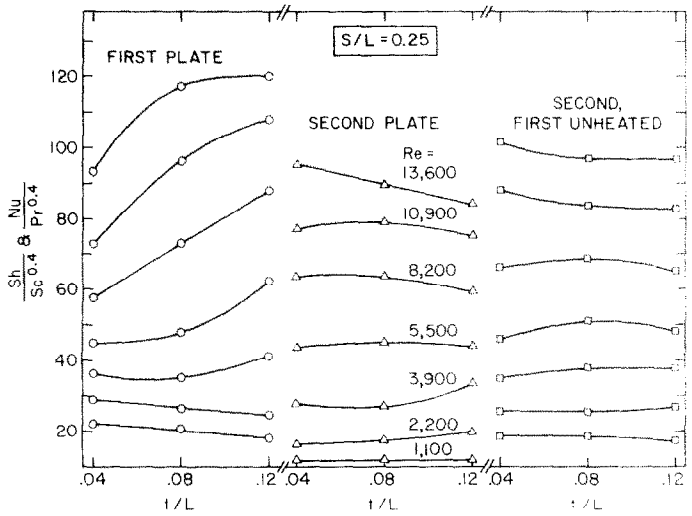

FIG. 6. Nusselt/Sherwood number variation with thickness ratio t/L; inter-plate spacing $S/L = 0.25$.

Although further perspectives will be available in later graphs, a brief comparison will be made here of the Nusselt number magnitudes for the first and second plates and for the different heating conditions. Consider first the case where both plates are heated. As expected, the deviations between the results for the first and second plates are generally greater at smaller spacings. For the smallest plate thickness, the second-plate Nusselt numbers tend to exceed those for the first plate at higher Reynolds numbers, with an opposite relationship at lower Reynolds numbers. This suggests that at the higher Re, the second plate benefits from being washed by the active wake of the first plate, but at lower Re it is penalized by being washed by already developed velocity and temperature distributions.

For the thicker plates, the second-plate Nusselt numbers are, for the most part, lower than those for the first plate. It thus appears that at higher Re, turbulence and eddies shed by the blunt leading edge of the first plate give rise to greater heat transfer augmentation than does the wake which washes the second plate. At lower Re, the second plate is again penalized by the developed velocity and temperature distributions spawned by the first plate.

The degree of responsiveness of the second-plate Nusselt number to the preheating of the air by the first plate can be assessed by comparison of the upper and middle sets of curves in Figs. 2–5. The absence of heat transfer at the first plate generally gives rise to an increase of the second-plate Nusselt number. The increases are most marked at low Reynolds numbers and at small inter-plate spacings. Thus, for example, for $S/L = 0.25$, $t/L = 0.04$, and $Re = 1100$ (Fig. 2), the second-plate Nusselt number increases by 59% when heating at the first plate is suppressed. For both of the aforementioned conditions, there is relatively little homogenization of the temperature field in the gap, so that the fluid arriving at the second plate has a clear memory of any preheating due to the first plate. Higher Reynolds numbers and larger gaps promote homogenization, with a corresponding reduction in the pre-heating effect.

Nusselt number–thickness ratio presentation

The Nusselt number/Sherwood number results will now be presented as a function of the thickness ratio t/L in Figs. 6–9, which correspond successively to spacing ratios S/L of 0.25, 0.5, 1, and 2. Each figure contains three columns of curves which represent the results for the first and second plates. For conciseness, the Reynolds numbers which parameterize the curves are listed only in the second column, but they are applicable for all of the cases.

These figures reaffirm that the thickness effect for the first plate is the same for all of the inter-plate spacings, that is, a substantial increase of the Nusselt number with thickness for higher Reynolds numbers and a modest decrease at lower Reynolds numbers.

The second plate Nusselt numbers corresponding to the smaller spacings are significantly less sensitive to thickness than are the first-plate Nusselt numbers, and the trends are not as regular. Thus, in the presence of a heated first plate, the second-plate Nusselt numbers for $S/L = 0.25$ tend to decrease moderately with thickness (except at the lower Reynolds numbers), whereas there is a tendency toward a moderate increase for $S/L = 0.5$. As the spacing increases, the higher Reynolds number results for the second plate tend to follow the thickness-related trends for the first plate, but with more moderate variations.

At lower Reynolds numbers, the second-plate Nusselt numbers (with heated first plate) generally increase with thickness at all spacings, which is just opposite to the trend for the first plate.

When the first plate is unheated, the second-plate Nusselt numbers for the smaller spacings continue to be relatively insensitive to thickness. At larger spacings, the trends tend to become indifferent to whether the first plate is heated or unheated.

With regard to heat exchanger applications, the $S/L = 1$ spacing ratio appears to be the most common. In that situation, and assuming that the second plate is more or less representative of multi-plate arrays, it can be concluded that thicker plates promote higher heat-transfer coefficients.

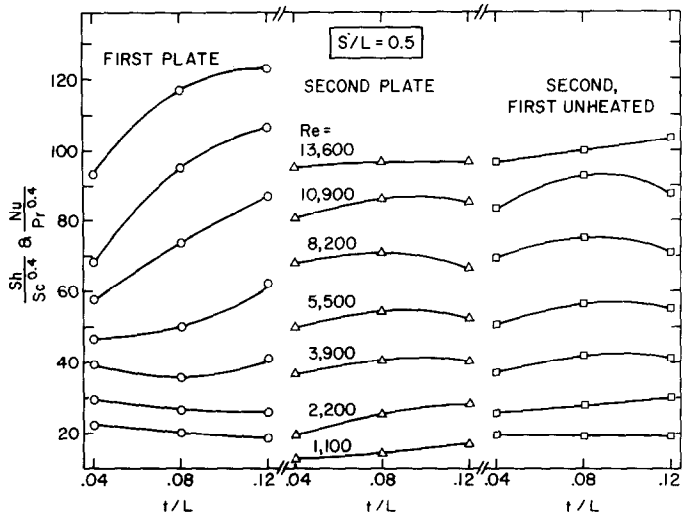

FIG. 7. Nusselt/Sherwood number variation with thickness ratio t/L; inter-plate spacing $S/L = 0.5$.

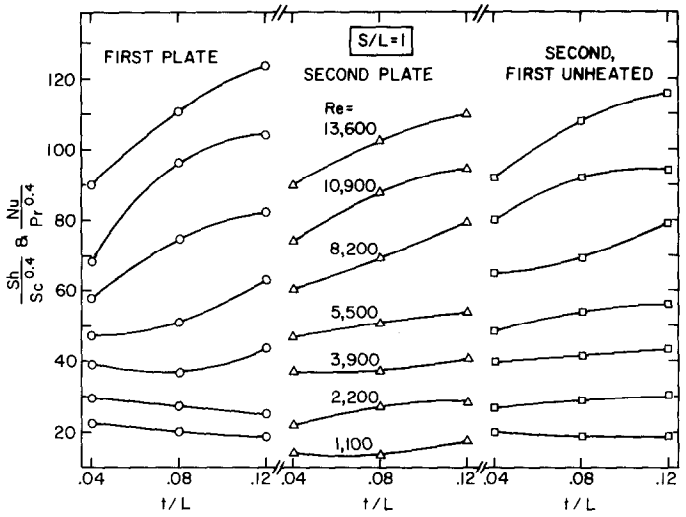

FIG. 8. Nusselt/Sherwood number variation with thickness ratio t/L; inter-plate spacing $S/L = 1$.

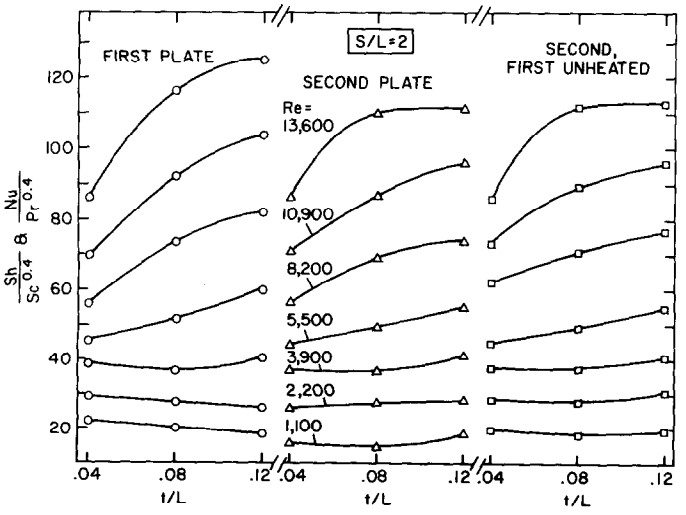

FIG. 9. Nusselt/Sherwood number variation with thickness ratio t/L; inter-plate spacing $S/L = 2$.

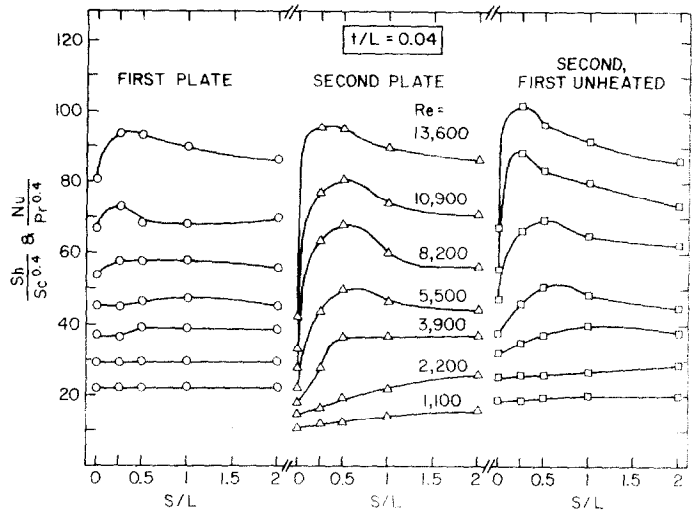

FIG. 10. Nusselt/Sherwood number variation with inter-plate spacing ratio S/L; thickness ratio $t/L = 0.04$.

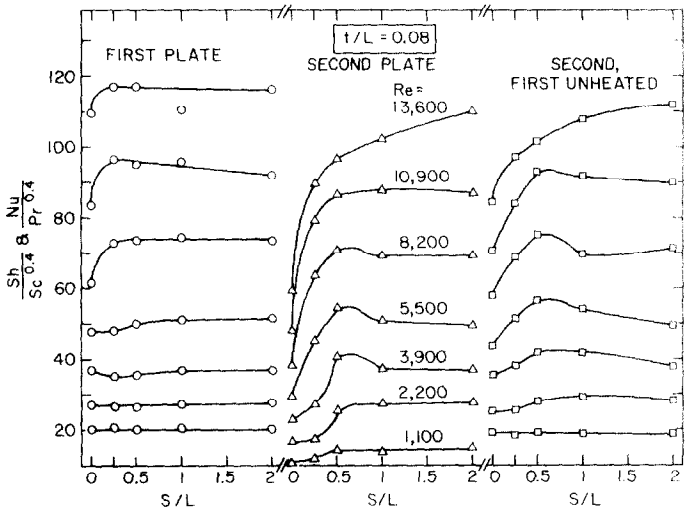

FIG. 11. Nusselt/Sherwood number variation with inter-plate spacing ratio S/L; thickness ratio $t/L = 0.08$.

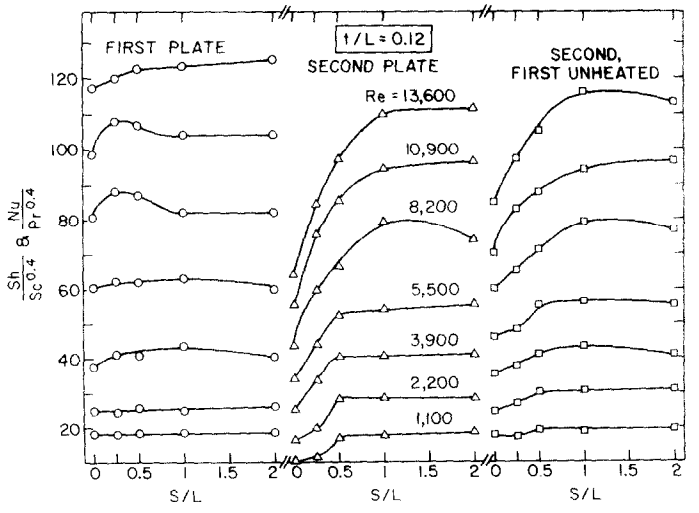

FIG. 12. Nusselt/Sherwood number variation with inter-plate spacing ratio S/L; thickness ratio $t/L = 0.12$.

Nusselt number–spacing ratio presentation

Attention will now be turned to identifying the response of the Nusselt number to variations of the inter-plate spacing. Relatively low values of the second-plate Nusselt number are expected as the spacing shrinks to zero, since the second plate then becomes an extension of the first plate and is washed by its (the latter's) boundary layers. On the other hand, when the spacing is large, relatively complete homogenization of the velocity and temperature fields should take place; the second-plate Nusselt numbers should be relatively large and insensitive to further increases in spacing. In addition, the visualization studies of [6] suggest that the flow field adjacent to the first plate can be affected by the magnitude of the inter-plate spacing, and this may affect the first-plate Nusselt numbers. With these expectations, the results will now be examined.

Figures 10–12 show the Nusselt and Sherwood numbers plotted as a function of the spacing ratio S/L for thicknesses t/L of 0.04, 0.08, and 0.12. These figures have a three-column structure which is the same as that already described in connection with Figs. 6–9. Aside from the realized expectations that the lowest Nusselt numbers occur at zero spacing and that there is a leveling-off tendency at larger spacings, the results display a complex variety of trends.

For the first plate, the Nusselt number is insensitive to spacing at the lower Reynolds numbers, indicating the absence of feedback from the wake. At larger Reynolds numbers, wake feedback is in evidence, as witnessed by the fact that the Nusselt number for the no-spacing case is smaller than those for finite spacings. For these Reynolds numbers, there appear to be two patterns in the curves of Nusselt number vs spacing. In one, the Nusselt number increases at first, attains a maximum, and then decreases and ultimately becomes constant. The maximum may well be due to a resonance phenomenon identified in [6]. In the other pattern, the Nusselt number increases and then levels off at a constant value. The existence of one or the other of the patterns does not appear to follow a regular rule.

For the second plate, the presence of an inter-plate gap generally augments the Nusselt number, but in a variety of patterns depending on the thickness ratio and the Reynolds number. At lower Reynolds numbers, the Nusselt number tends to level off after an initial rise. At higher Reynolds numbers, there are cases, especially at small and intermediate thicknesses, where the Nu vs S/L curve displays an overshoot. For other cases, the overshoot is absent. The trends with S/L do not appear to be markedly affected by whether the first plate is heated or unheated.

It is difficult to discern a clear pattern in the presence or absence of overshoot. Furthermore, in certain cases, overshoot is present for the second-plate Nusselt number but not for the first-plate Nusselt number, suggesting that the causal phenomena are not necessarily the same. It is likely that an important contributor to the second-plate overshoot is the high level of the velocity fluctuations in the inter-plate gap that occur at specific spacings [6].

If it were a heat exchanger design objective to choose a spacing which yields the highest possible Nusselt number, then some consideration would have to be given to the plate thickness and to the Reynolds number range. For relatively thick plates, the conventional $S/L = 1$ appears to be suitable, as it is for low Reynolds numbers for thinner plates. However, for those parameter values where there is second-plate overshoot, smaller spacings, say $S/L = 0.5$, appear to be more appropriate.

Comparisons

It is relevant to consider comparisons between the present results and those of [5]. Such comparisons are necessarily constrained because, as noted in the Introduction, the ranges of S/L and t/L investigated in [5] were too small to permit trends to be determined.

A comparison of the heat- (mass-) transfer results is made in Fig. 13 for the spacing ratio $S/L = 1$. Here, in conformity with [5], the Stanton number St has been used to portray the transfer coefficients, and the Reynolds number Re_L based on the plate length L is the abscissa. The three groups of curves shown in the figure are respectively for the first plate, second plate, and second plate with unheated first plate. The plate thickness appears as a parameter on the curves and, in this connection, it is important to note that the t/L values for the two experiments do not coincide.

Inspection of Fig. 13 indicates that the trends from the two sets of experiments are the same, but there are some differences in the level of the transfer coefficients. Part of the difference can be ascribed to the aforementioned non-coincidence of the thicknesses of the plates. Also of significance is the probable difference in the level of the free stream turbulence in the flow approaching the first plate. In addition, there are other

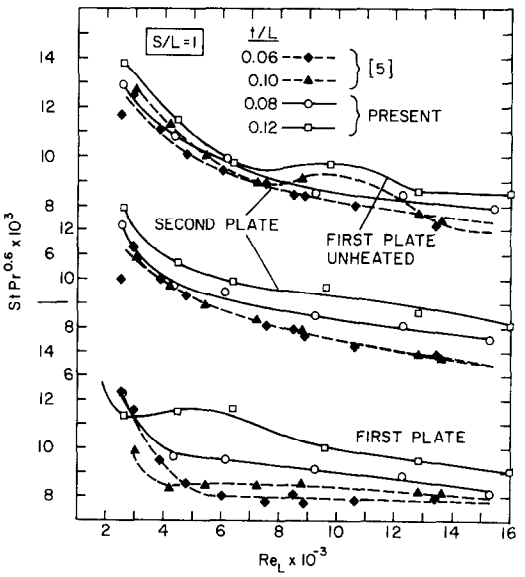

FIG. 13. Comparison of present heat/mass-transfer results with those of [5].

uncertainties that stem from the fact that the plotted second-plate data points of [5] were not directly measured but were inferred from other measurements. A further cause for uncertainty is that it is not known whether the velocity used to evaluate Re_L in [5] is that upstream of the plates or in the space above or below the plates. In light of these considerations, it is felt that the comparison of results is entirely satisfactory.

Pressure drop

Axial pressure distributions were measured for each data run, and a typical distribution is shown in Fig. 14.

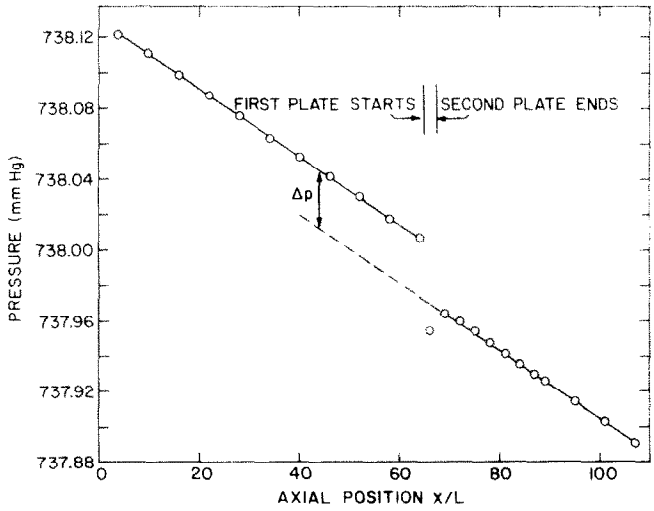

FIG. 14. Representative axial pressure distribution ($Re = 8200$, $t/L = 0.12$, $S/L = 0.5$).

It is seen from the figure that hydrodynamic development is attained both upstream and downstream of the two-plate array, as witnessed by the linear variation of p vs x/L. Although the slopes of the upstream and downstream straight lines are the same, they are displaced owing to the pressure loss which occurs due to the presence of the plates. This vertical displacement between the curves is denoted by Δp.

Working graphs such as Fig. 14 were prepared for all of the data runs and the Δp values were thus determined. For a dimensionless presentation, the ratio $\Delta p/\frac{1}{2}\rho\bar{V}^2$ was evaluated, where $\bar{V}$ is the mean velocity in the space above or below a plate. To conserve space, an abbreviated listing of $\Delta p/\frac{1}{2}\rho\bar{V}^2$ is given here, with a fuller presentation in [7].

From the table, it is seen that the dimensionless pressure drop increases substantially with thickness. These increases in pressure drop are larger, percentagewise, than the largest thickness-related increase in the Nusselt number. The relative insensitivity of the pressure drop to the magnitude of the inter-plate spacing is noteworthy and is somewhat surprising since the flow pattern depends on the spacing. This insensitivity enables the spacing to be selected on the basis of heat-transfer considerations, consistent, of course, with fabrication and other mechanical design constraints. There is a general trend toward higher values of $\Delta p/\frac{1}{2}\rho\bar{V}^2$ at lower Reynolds numbers which is in accordance with all prior experience for duct flows (e.g. f vs Re).

CONCLUDING REMARKS

On the basis of the experimental results, the response of the Nusselt/Sherwood number for each plate of a two-plate array to variations in Reynolds number, thickness, and spacing can be identified. For the first plate, the Nusselt number increases substantially with thickness at the higher Reynolds numbers but decreases moderately with thickness at the lower Reynolds numbers. The second-plate Nusselt numbers are relatively insensitive to thickness at smaller spacings but become more sensitive as the spacing increases. Since the spacing $S/L = 1$ is typical of heat exchangers and if the second plate is assumed to be more or less representative of a multi-plate array, then it can be concluded that thicker plates promote higher heat-transfer coefficients in such devices.

For thicker plates, the second-plate Nusselt number is, for the most part, lower than the first-plate Nusselt number, whereas for thin plates it may be higher or lower depending on the Reynolds number. The effect of suppressing heating at the first plate is to increase the second-plate Nusselt number. The increases are most marked at lower Reynolds numbers and smaller inter-plate spacings.

The presence of an inter-plate gap, relative to no gap, affects both the first- and second-plate Nusselt numbers, but to a lesser extent for the former (with no effect at the lower Reynolds numbers). The Nusselt number vs spacing curves display two patterns. In one, the Nusselt number increases at first, attains a maximum, and then diminishes towards a constant value. In the other, the Nusselt number increases

Table 1. Pressure drop $\Delta p/\frac{1}{2}\rho\bar{V}^2$ due to two-plate array

		t/L		
Re	S/L	0.04	0.08	0.12
2200	0.25	0.146	0.195	0.276
	0.5	0.149	0.187	0.289
	1	0.146	0.207	0.309
	2	0.150	0.204	0.293
8200	0.25	0.107	0.167	0.226
	0.5	0.104	0.195	0.230
	1	0.118	0.188	0.257
	2	0.120	0.193	0.256
13 600	0.25	0.078	0.151	0.190
	0.5	0.105	0.151	0.214
	1	0.099	0.159	0.226
	2	0.103	0.164	0.225

monotonically and then levels off. In those cases where the curve has a maximum, the use of the conventional $S/L = 1$ spacing corresponds to a Nusselt number lower than the maximum.

The pressure drop increase caused by increasing plate thickness is greater than the largest thickness-related increase of the Nusselt number. On the other hand, the pressure drop is relatively insensitive to the inter-plate spacing.

Acknowledgement—This research was performed under the auspices of ONR Contract N00014-76-C-0246.

REFERENCES

1. A. R. Wieting, Empirical correlation for heat transfer and flow friction characteristics of rectangular offset-fin plate-fin heat exchangers, *J. Heat Transfer* **97**, 488–490 (1975).
2. R. K. Shah, Perforated heat exchanger surfaces. Part 2—heat transfer and flow friction characteristics, ASME paper 75-WA/HT-9, Am. Soc. Mech. Engrs, New York (1975).
3. R. K. Shah and A. L. London, Offset rectangular plate-fin surfaces—heat transfer and flow friction characteristics, *J. Engng Power* **90**, 218–228 (1968).
4. W. M. Kays and A. L. London, *Compact Heat Exchangers*, 2nd edn. McGraw-Hill, New York (1964).
5. D. B. Adarkar and W. M. Kays, Heat transfer in wakes, Technical Report No. 55, Department of Mechanical Engineering, Stanford University, Stanford, California (1963).
6. R. I. Loehrke, R. E. Roadman and G. W. Reed, Low Reynolds number flow in plate wakes, ASME paper 76-WA/HT-30, Am. Soc. Mech. Engrs, New York (1976).
7. N. Cur, Experiments on heat transfer and pressure drop for an array of colinear interrupted plates, Ph.D. Thesis, Department of Mechanical Engineering, University of Minnesota, Minneapolis, Minnesota (1978).
8. H. H. Sogin, Sublimation from disks to air streams flowing normal to their surfaces, *Trans. Am. Soc. Mech. Engrs* **89**, 61–79 (1958).
9. B. S. Petukhov, Heat transfer and friction in turbulent pipe flow with variable physical properties, *Adv. Heat Transfer* **6**, 523 (1972).

EXPERIENCES SUR LE TRANSFERT THERMIQUE ET LA PERTE DE CHARGE POUR UNE PAIRE DE PLAQUES COLINEAIRES ALIGNEES AVEC L'ECOULEMENT

Résumé—On a déterminé expérimentalement les caractéristiques du transfert de chaleur pour chaque plaque d'un arrangement colinéaire de deux plaques, parallèle à la direction de l'écoulement d'air et situé dans un conduit rectangulaire et aplati. La chute de pression associée est déterminée. L'épaisseur de plaque et l'espace entre plaques sont des paramètres variables (pour une longueur de plaque donnée) ainsi que le nombre de Reynolds. On a trouvé que tandis que le nombre de Nusselt peut soit croître, soit décroître avec l'épaisseur de plaque suivant les conditions opératoires, il croît dans les conditions correspondant à celles généralement rencontrées dans un échangeur à plaque interrompue. L'augmentation de la chute de pression due à l'accroissement de l'épaisseur de plaque est supérieure à l'augmentation du nombre de Nusselt. La présence de l'espace entre plaques affecte les nombres de Nusselt de la première comme de la seconde plaque, mais avec plus de poids pour cette dernière. Dans de nombreux cas, les courbes de variation du nombre de Nusselt en fonction de cet espace atteignent un maximum local et indiquent que le rapport espace-sur-longueur conventionnellement égal à l'unité n'est pas nécessairement optimal.

MESSUNGEN DES WÄRMEÜBERGANGS UND DRUCKABFALLS AN EINEM PAAR UNTERBROCHENER PLATTEN, DIE IN STRÖMUNGSRICHTUNG FLUCHTEND ANGEORDNET SIND

Zusammenfassung—Zur Bestimmung des Wärmeübergangs an jeder Platte der zwei hintereinander angeordneten Plattenpaare wurden Versuche durchgeführt, wobei sich die Platten im Luftstrom in einem rechteckigen Kanal befanden. Der dabei auftretende Druckabfall wurde ebenfalls bestimmt. Die Plattendicke und der Zwischenplattenabstand wurden bei verschiedenen Reynolds-Zahlen (bei fester Plattenlänge) variiert. Es wurde festgestellt, daß die Nusselt-Zahl mit der Plattendicke zu- oder abnimmt, abhängig von den Arbeitsbedingungen, während zu erwarten ist, daß die Nusselt-Zahl zunehmen müßte. Die Zunahme des Druckabfalls ist größer als die größte Zunahme der Nusselt-Zahl. Die vorhandene Unterbrechung der Platten beeinflußt sowohl den Wärmeübergang an der ersten als auch an der zweiten Platte, wobei der Einfluß auf die zweite Platte stärker ist. In vielen Fällen erreichen die Kurven für die Nusselt-Zahl in Abhängigkeit vom Plattenlängsabstand ein Maximum, und es zeigt sich, daß das konventionelle Verhältnis der Plattenlängsteilung von eins nicht unbedingt optimal ist.

ЭКСПЕРИМЕНТАЛЬНОЕ ИССЛЕДОВАНИЕ ТЕПЛООБМЕНА И СОПРОТИВЛЕНИЯ ПАРЫ КОЛЛИНЕАРНЫХ ПЛАСТИН, ОРИЕНТИРОВАННЫХ ПО ПОТОКУ

Аннотация — Проведено экспериментальное исследование характеристик переноса тепла для каждой из пары коллинеарных пластин, расположенных параллельно потоку воздуха в плоском прямоугольном канале. Определялось также падение давления на пластинах. В опытах изменялись толщина пластин и расстояние между ними (при постоянной их длине), а также число Рейнольдса. Найдено, что при изменении толщины пластины число Нуссельта может как увеличиваться, так и уменьшаться в зависимости от режимных параметров. Число Нуссельта увеличивается для режимных параметров, соответствующих тем, которые обычно наблюдаются в теплообменниках с продольно-прерывистым оребрением. С ростом толщины пластины увеличение падения давления больше, чем наибольшее увеличение числа Нуссельта. Зазор между пластинами влияет на значение числа Нуссельта как для первой, так и для второй пластины, но в большей степени для второй. Для многих режимов кривые зависимости числа Нуссельта от величины зазора достигают локального максимума, что свидетельствует о том, что обычное отношение величины зазора к длине пластин, равное единице, не обязательно является оптимальным.